PCCP

PAPER

View Article Online
View Journal | View Issue

Cite this: *Phys. Chem. Chem. Phys.*, 2024, **26**, 11482

Doubly charged dimers and trimers of heavy noble gases†

Gabriel Schöpfer, ‡[a] Stefan Bergmeister, ‡[a] Milan Ončák, *[a] Ianessa Stromberg, [ab] Masoomeh Mahmoodi-Darian, [a] Paul Scheier, [a] Olof Echt *[ac] and Elisabeth Gruber [a]

Received 31st January 2024,
Accepted 21st March 2024

DOI: 10.1039/d4cp00465e

rsc.li/pccp

Many doubly charged heteronuclear dimers are metastable or even thermodynamically stable with respect to charge separation. Homonuclear dicationic dimers, however, are more difficult to form. He_2^{2+} was the first noble gas dimer predicted to be metastable and, decades later, observed. Ne_2^{2+} is the only other dicationic noble gas dimer that has been detected so far. Here, we present a novel approach to form fragile dicationic species, by post-ionization of singly charged ions that are embedded in helium nanodroplets (HNDs). Bare ions are then extracted by colliding the HNDs with helium gas. We detect homonuclear doubly charged dimers and trimers of krypton and xenon, but not argon. Our multi-reference *ab initio* calculations confirm the stability of Kr_2^{2+}, Kr_3^{2+}, Xe_2^{2+}, Xe_3^{2+}, and Ar_2^{2+}, but put the stability of Ar_3^{2+} towards dissociation to $Ar^+ + Ar_2^+$ into question.

1 Introduction

In 1933, Pauling postulated the existence of metastable He_2^{2+}.[1] He calculated that the local minimum lies more than 10 eV above the separated $He^+ + He^+$ ion pair at an internuclear distance of 0.75 Å and supports 4 vibrational states. It took five decades until He_2^{2+} could be prepared by charge stripping of He_2^+.[2,3] The observation was indirect, only showing the He^+ fragments, but in later experiments He_2^{2+} with a lifetime exceeding 5 μs could be identified.[4]

A few years later, Ne_2^{2+} was detected in charge-stripping collisions of Ne_2^+ with Ar, and by field desorption.[5,6] A lifetime of at least 1 μs was inferred. The results were puzzling because theoretical work shows that the $^1\Sigma_g^+$ ground state of Ne_2^{2+} is purely repulsive.[7–9]

Several experimental and theoretical reports have been devoted to the heavier noble gases (Ng).[10] Argon clusters are a model system for the study of interatomic coulombic decay (ICD). When a core electron is removed from an atom in Ar_2, the hole may be filled by a valence electron and the excess energy causes the emission of another valence electron (a so-called Auger–Meitner electron), resulting in $Ar–Ar^{2+}$. Alternatively, in the ICD process,[11,12] the energy released upon filling the hole is transferred to a valence electron in the other atom, resulting in $Ar^+–Ar^+$.

ICD in argon clusters has been investigated by measuring the kinetic energy of the emitted electrons, ions, and by electron–ion and ion–ion coincidence experiments. The presence of a fleeting Ar_2^{2+} has been inferred from the observation of high-energy fragment ions but intact Ar_2^{2+} has never been detected.[12–20] Ar_2^{2+} has a local minimum in the potential energy curve (PEC) at about 2 Å but this quasi-bound region cannot be reached by vertical ionization of Ar_2 which has an internuclear distance of 3.76 Å.[21–23]

The processes following core-level excitation in krypton and xenon clusters have been studied by similar techniques.[23–27] Again, the existence of transient dicationic dimers Ng_2^{2+} has been inferred from the data but intact Ng_2^{2+} was not observed. Doubly charged noble gas dimers are also of interest because they may give rise to the so-called third excimer continuum in the VUV emission spectra of the noble gases.[27]

Here we explore a novel method to form dications of van der Waals bound systems. As shown recently, fragile ionic species such as SF_6^+ or the phenanthrene anion Ph^- can be synthesized in and gently extracted from helium nanodroplets (HNDs).[28–30] We have added a second ionizer to the experimental apparatus, making it possible to form dications by sequential ionization.[31] Vertical ionization of a singly-charged molecular ion offers a much better chance to reach the metastable dicationic state than vertical ionization of a neutral molecule.[21]

With this novel approach[31] we are able to detect long-lived Kr_2^{2+} and Xe_2^{2+} in a high-resolution mass spectrometer.

[a] *Institut für Ionenphysik und Angewandte Physik, Universität Innsbruck, Innsbruck, Austria. E-mail: Milan.Oncak@uibk.ac.at, Olof.Echt@unh.edu*
[b] *School of Chemistry, University of Edinburgh, Edinburgh, UK*
[c] *Department of Physics, University of New Hampshire, Durham, USA*

† Electronic supplementary information (ESI) available: Mass spectra of Kr with and without the second ionizer, benchmarking and definition of the active spaces for dicationic dimers and trimers, contour plots for dissociation of Kr_3^{2+} and Xe_3^{2+}. See DOI: https://doi.org/10.1039/d4cp00465e

‡ The authors contributed equally.

We also observe doubly-charged trimers, but no tetramers. Similar experiments with argon do not produce small dicationic species but this failure may be due to technical challenges. Our experiments are supported by *ab initio* calculations that quantify the respective Coulomb barriers and confirm Ar_2^{2+} as a metastable ion but predict Ar_3^{2+} to dissociate spontaneously into $Ar_2^+ + Ar^+$.

2 Methods

2.1 Experimental details

An earlier version of the apparatus[32] was recently upgraded by the implementation of a second electron impact ionizer.[31] HNDs containing some 10^6 atoms are produced in an expansion of helium gas through a 5 μm nozzle into vacuum. Interaction with an intense 40 eV electron beam introduces a few to a few dozen positive charges into the HND,[33] resulting in He_N^{z+} nanodroplets that contain z molecular helium ions, probably He_3^+.[34,35] The ions reside near the surface of the HND because of mutual coulombic repulsion.[36] The He_N^{z+} nanodroplets are passed through an electrostatic deflector which selects them by their mass-to-charge ratio, hence their size-to-charge ratio N/z, and are then guided through a pickup cell filled with a low-density noble gas. Captured Ng atoms agglomerate in the HNDs at the charge centers and form z singly charged clusters Ng_n^+.

The ion beam is intersected by another intense electron beam at 40 eV which introduces additional charges in the droplets. It will also electronically excite helium. The electronic excitation may find its way to the dopant and Penning ionize Ng_n^+ to Ng_n^{2+}.[35,37–39] The HNDs are then collided with helium gas in an ion guide, leading to the gentle escape of the dopant ions from the droplet. Their mass-to-charge ratio m/z is determined in a time-of-flight mass spectrometer (TOF-MS) equipped with an electrostatic reflectron. The mass resolution is about 10^4 full-width at half-maximum.

2.2 Computational details

The challenge in computational treatment of doubly-charged rare gas dimers and trimers is the metastability evolving from the competition between the covalent bond formed at short distances and the Coulomb repulsion between nuclei destabilizing the system (Scheme 1). Here, we use both single-reference and multi-reference methods to describe the electronic structure of the metastable ions. Namely, we employ the coupled cluster singles and doubles with non-iteratively included triplets (CCSD(T)) and multi-reference configuration interaction singles and doubles (MRCI) based on complete active space self-consistent field (CASSCF). Single-reference CCSD(T) calculations are employed for calculating the dissociation energy while MRCI is used to describe the Coulomb barrier. Both methods are used to predict the metastable minima.

The active space size is a crucial parameter in multi-reference calculations. Detailed active space benchmarking, orbital composition of various active spaces and included electronic states can be found in the ESI,† Fig. S2–S5 and Tables S1–S4. Here, we only summarize the respective conclusions. The Ng_2^{2+} and Ng_3^{2+} ions are calculated as linear, corresponding to $D_{\infty h}$ and $C_{\infty v}$ point groups lowered to D_{2h} and C_{2v} point groups, respectively, in actual MRCI calculations. For Ng_2^{2+}, we included six orbitals correlated to valence p orbitals in Ng^+ (σ_g^+, σ_u^+, π_g, π_u) with 10 electrons, and gradually increased the active space by including more virtual orbitals, finally employing 10 electrons in 11 orbitals, (10,11). For the full electronic state analysis of Ar_2^{2+}, we included all 36 states which correlate with the Ar (^{2}P) + Ar (^{2}P) asymptote, namely 9 singlet (2x $^1\Sigma_g^+$, $^1\Pi_g$, $^1\Delta_g$, $^1\Sigma_u^-$, $^1\Pi_u$) and 27 triplet ($^3\Sigma_g^-$, $^3\Pi_g$, 2x $^3\Sigma_u^+$, $^3\Pi_u$, $^3\Delta_u$) electronic states. For the scans, we included 5 singlet ($^1\Sigma_g^+$, $^1\Pi_g$, $^1\Pi_u$) and 12 triplet ($^3\Pi_g$, $^3\Pi_u$) electronic states. In Ng_3^{2+}, we included 16 electrons in 9 valence orbitals (σ_g^+, 2x σ_u^+, π_g, 2x π_u), again enlarging the active space with further virtual orbitals in the second step. In the main text, results of (16,9) and (16,10) active spaces are compared. We included

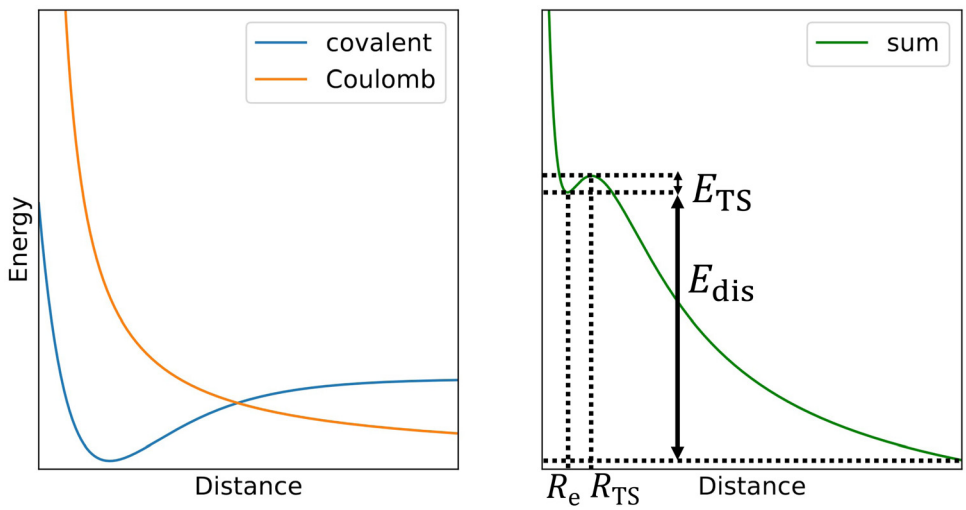

Scheme 1 In the first approximation, the potential energy curve for dissociation of doubly-charge ions (right) can be thought as a sum of a covalent bond potential and Coulomb repulsion (left).

5 singlet ($^1\Sigma_g^+$, $^1\Pi_g$, $^1\Pi_u$) and 15 triplet ($^3\Pi_g$, $^3\Sigma_u^+$, $^3\Pi_u$) electronic states. For the 2D scans in the lower $C_{\infty v}$ symmetry, we used the orbitals and electronic states corresponding to the ones in the $D_{\infty h}$ calculations. We note that empirical Davidson correction to estimate the influence of higher-order excitations influences somewhat the dissociation barriers as shown in the ESI† (Fig. S2, S3 and S5).

The zero-point correction in dissociation energies is included as calculated at the CCSD level, no zero-point correction is used for calculating Coulomb barriers. Within single-reference calculations, restricted Hartree–Fock (HF) wave functions are used for singlet species. In Ng_3^{2+} ions, stabilization of the electronic wave function in the HF calculation leads to an unrestricted wave function with lower HF and CCSD energies, predicting no metastable minimum for Ar_3^{2+} and Kr_3^{2+}. This further emphasizes the complex electronic structure of the species. In all calculations, the def2QZVPPD basis set is employed. The Gaussian software is used for single-reference calculations,[40] Molpro for multi-reference ones.[41,42]

3 Results

Fig. 1 displays a mass spectrum of HNDs doped with Kr. The prominent mass peaks in panel a (recorded with both ionizers turned on, note the logarithmic *y*-scale) are due to Kr isotopes $^{78}Kr^+$ through $^{86}Kr^+$. Their natural abundance distribution is indicated by the dashed line. The line describes the observed ion yield quite well. Mass peaks due to Kr_2^{2+} with an even mass number cannot be distinguished from those due to singly charged monomers, but they can be identified if their nominal mass is an odd integer. Mass peaks due to $^{80}Kr^{83}Kr^{2+}$, $^{82}Kr^{83}Kr^{2+}$, $^{84}Kr^{83}Kr^{2+}$, and $^{86}Kr^{83}Kr^{2+}$ are, indeed, clearly seen. The expected abundance distribution of the isotopologues of Kr_2^{2+}, indicated by the dash-dotted line, agrees well with the data when m/z is half-integer.

The mass spectrum in Fig. 1b covers the same m/z range as in Fig. 1a. It was recorded with the second ionizer turned off. As expected, no ions appear at half-integer m/z values. The spectrum in Fig. 1c (recorded with both ionizers on) covers the range where doubly charged trimers would appear. Indeed, we observe three mass peaks at half-integer m/z values. Each of these peaks has contributions from several isotopologues whose exact m/z values differ by less than ≈ 0.002. The individual peaks cannot be resolved, but the expected cumulative abundance distribution describes the measured peak heights well. The half-integer mass peaks in Fig. 1c disappear when the second ionizer is turned off, see the ESI† (Fig. S1). The prominent mass peaks in Fig. 1c at integer m/z are mostly due to He_mKr^+. These complexes also account for the strong mass peaks at m/z = 87 and 88 in Fig. 1a and b.

A mass spectrum of HNDs doped with Xe, recorded with both ionizers turned on, is presented in Fig. 2. The isotopes of Xe, ^{128}Xe through ^{136}Xe, give rise to the prominent mass peaks in panel a (note the break in the *y*-scale). Several mass peaks appear at half-integer m/z values, starting at 130.5 which is

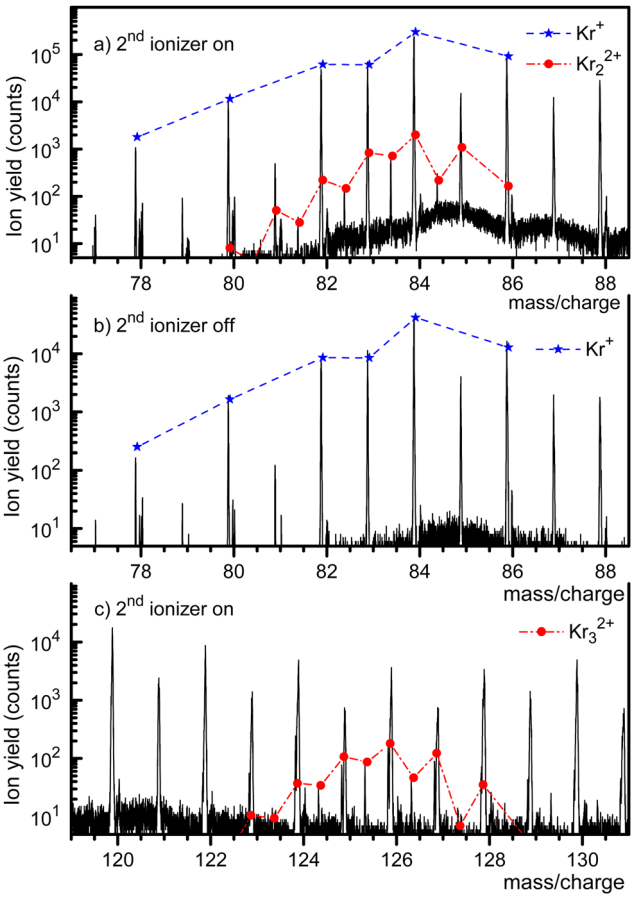

Fig. 1 A mass spectrum of HNDs doped with Kr reveals the existence of Kr_2^{2+} and Kr_3^{2+} when both ionizers are turned on (panels a and c, respectively). The expected abundance distributions of their isotopologues are indicated by dash-dotted lines. Only singly charged Kr ions are seen when the second ionizer is turned off (panel b).

mostly due to $^{129}Xe^{132}Xe^{2+}$ plus a small contribution from $^{130}Xe^{131}Xe^{2+}$. The expected abundance distribution, scaled to the value observed at m/z = 130.5, is shown by the dash-dotted line. The line underestimates the height of mass peaks further to the right, presumably because of contributions from $He_mXe_2^{2+}$. Likewise, the mass peaks in Fig. 2a at m/z = 133, 135, 137 and 138 are due to He_mXe^+. It is impossible to set the pressure in the collision cell where He is stripped from the HNDs such that the embedded ions are completely stripped of the He without dissociating the bare dimers or trimers.

The half-integer mass peaks in Fig. 2b are due to the isotopologues of Xe_3^{2+}. The mismatch between the expected distribution of its isotopologues and the observed peak heights beyond $m/z \approx 196$ indicates contributions from $He_mXe_3^{2+}$. On the other hand, there is no discernible contribution from He_mXe^+ ions in this m/z range.

Now we turn to the computational investigation of the metastable ions. Somewhat simplified, the Coulomb barrier E_{TS} towards dissociation of doubly charged ions can be thought to arise due to the combination of a covalent bond potential with the Coulomb repulsion (Scheme 1; see ref. 9 for a detailed

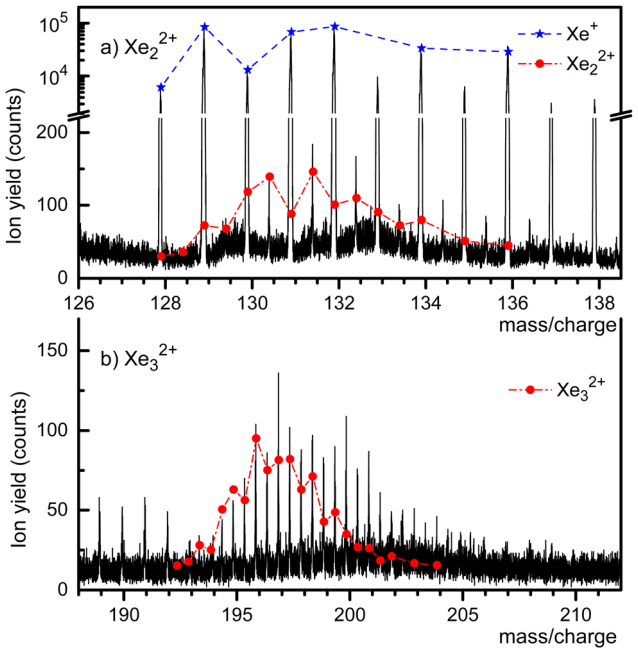

Fig. 2 Sections of a mass spectrum of HNDs doped with Xe, with both ionizers turned on. Doubly charged dimers and trimers are observed in panels a and b, respectively. The expected abundance distributions are indicated by dash-dotted lines. Mass peaks at half-integer m/z values that are more intense than expected are due to $He_mXe_n^{2+}$ complexes.

discussion of various contributing effects). The respective bound state is then often metastable towards dissociation, with the overall dissociation energy of E_{dis}.

All investigated doubly-charged Ng_2^{2+} ions, Ng = Ar, Kr, Xe, were found to be metastable with respect to dissociation into two Ng^+ (^2P) ions. Table 1 lists selected calculated properties of the ions at CCSD(T) and MRCI levels of theory; both methods predict the same optimal bond lengths within 0.012 Å. The intranuclear distance increases from about 2.02 Å for Ar_2^{2+} through 2.32 Å for Kr_2^{2+} to 2.69 Å for Xe_2^{2+}. A larger distance between nuclei leads to lower Coulomb repulsion as can be also seen from the dissociation energy to form $Ng^+ + Ng^+$ that is predicted as 4.75 eV (Ar_2^{2+}), 3.95 eV (Kr_2^{2+}) and 3.18 eV (Xe_2^{2+}).

While the dissociation energy is relatively straightforward to calculate, the barrier against dissociation is harder to assess. The electronic structure of the Ar_2^{2+} ion is analyzed in Fig. 3a. There are 36 electronic states corresponding to the asymptote of Ar^+ (^2P) + Ar^+ (^2P). Among these, only one $^1\Sigma_g^+$ molecular term is bound at a short internuclear distance while all other terms ($^1\Sigma_g^+$, $^1\Sigma_u^-$, $^1\Pi_g$, $^1\Pi_u$, $^1\Delta_g$, $^3\Sigma_g^-$, 2x $^3\Sigma_u^+$, $^3\Pi_g$, $^3\Pi_u$, $^3\Delta_u$) correspond to purely dissociative states, analogously to the situation in the isoelectronic Cl_2 system.[43] The potential energy curves in Fig. 3a illustrate the inherent problem in modeling the Coulomb barrier in Ng_2^{2+} ions. In the vicinity of the transition state that arises as a combination of the covalent bond potential and the Coulomb interaction, the curve of the $^1\Sigma_g^+$ term is crossed by the dissociative states. Single-reference methods might struggle to describe this region and, therefore, multi-reference approach was used for calculating the Coulomb barriers.

Table 1 Calculated properties of Ng_2^+, Ng_2^{2+}, Ng_3^+, and Ng_3^{2+} including dissociation of the doubly-charged species into $Ng^+ + Ng^+$ and $Ng_2^+ + Ng^+$. See Scheme 1 for definition of the used nomenclature. The def2QZVPPD basis set was used for all calculations, see Methods for further details. Bond lengths in Ng_2 are added for comparison

	Ar	Kr	Xe
R_e (Ng_2)/Å, ref. 51	3.758	4.03	4.361
R_e (Ng_2^+)/Å, CCSD(T)	2.408	2.698	3.073
R_e (Ng_2^{2+})/Å, CCSD(T)	2.026	2.324	2.688
R_e (Ng_2^{2+})/Å, MRCI(10,11)	2.014	2.325	2.697
R_{TS} (Ng_2^{2+})/Å, MRCI(10,11)	2.581	3.011	3.547
E_{TS} (Ng_2^{2+})/eV, MRCI(10,11)	0.42	0.50	0.59
E_{dis} (Ng_2^{2+})/eV, CCSD(T)	4.75	3.95	3.18
R_e (Ng_3^+)/Å, CCSD(T)	2.58	2.87	3.25
R_e (Ng_3^{2+})/Å, CCSD(T)	2.35[a]	2.58	2.91
R_e (Ng_3^{2+})/Å, MRCI(16,9)	—	2.65	2.97
R_e (Ng_3^{2+})/Å, MRCI(16,10)	—	2.62	2.96
R_{TS} (Ng_3^{2+})/Å, MRCI(16,9)	—	3.08; 2.93	3.74; 3.21
R_{TS} (Ng_3^{2+})/Å, MRCI(16,10)	—	3.14; 2.84	3.78; 3.17
E_{TS} (Ng_3^{2+})/eV, MRCI(16,9)	—	0.058	0.22
E_{TS} (Ng_3^{2+})/eV, MRCI(16,10)	—	0.12	0.28
E_{dis} (Ng_3^{2+})/eV, CCSD(T)	3.51	2.88	2.24

[a] A minimum is predicted with a barrier of 0.07 eV towards dissociation into Ar_2^+ and Ar^+.

Our MRCI calculations predict almost the same barrier against dissociation of 0.4–0.6 eV for all three Ng_2^{2+} ions, the bond length in the transition state is by about 30% longer than in the metastable minimum. In the dissociation curves in Fig. 3b–d, the turn in the curve between the regions of covalent bonding and Coulomb dissociation is clearly visible; the active spaces include all orbitals correlating to p orbitals of Ng^+ and seem to be converged with respect to the number of virtual orbitals (see also the ESI†).

In doubly-charged trimers, Ng_3^{2+}, the minimum is predicted to be a linear structure of $D_{\infty h}$ symmetry, in agreement with a previous study on He_3^{2+}.[44] While Kr_3^{2+} and Xe_3^{2+} ions are predicted to be metastable towards dissociation into $Ng^+ + Ng_2^+$, our calculations are not unequivocal with respect to stability of Ar_3^{2+}. At the CCSD(T) level, a minimum is predicted with the bond length of 2.35 Å (Table 1), with a barrier towards dissociation of 0.07 eV, above the calculated zero-point energy of the symmetric stretch mode of 0.014 eV. At the MRCI level, none of the investigated active spaces predicts a minimum along the Ar–Ar–Ar dissociation coordinate (Fig. 4a). The *a posteriori* Davidson correction (MRCI + Q) predicts a minimum with a barrier against symmetric dissociation of about 0.05 eV (Fig. S5, ESI†). While the MRCI approach might be still considerably influenced by the active space size and the absence of proper treatment of triples and higher excitations, the CCSD(T) method might suffer from an inappropriate Hartree–Fock wave function used as the basis of the calculation; it is therefore complicated to give a definitive verdict on Ar_3^{2+} (in)stability.

In Kr_3^{2+} and Xe_3^{2+}, optimal bond lengths at MRCI and CCSD(T) levels differ by about 0.1 Å, *i.e.*, considerably more than in Ng_2^{2+} systems, hinting towards a more involved electronic structure. The transition state for dissociation to $Ng_2^+ + Ng^+$ is asymmetric (Fig. 4b and c), reflecting the formation of the Ng_2^+ ion along the reaction pathway. Dissociation takes place

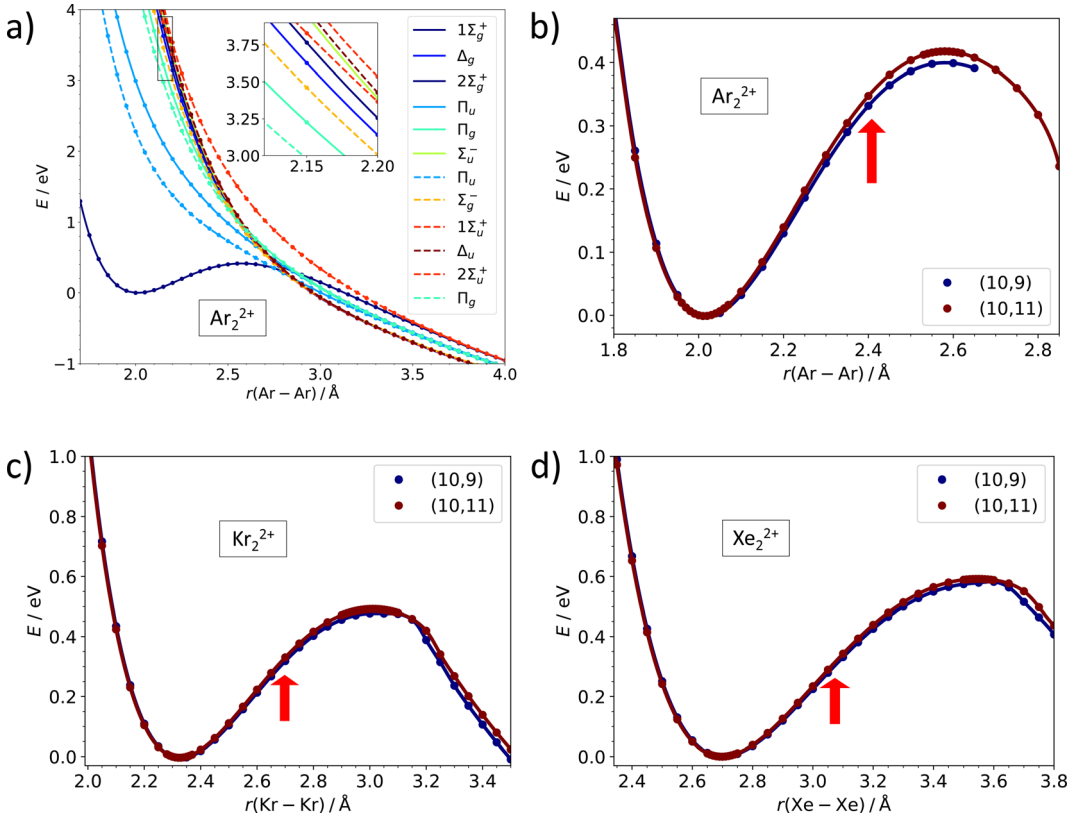

Fig. 3 Multi-reference calculations on Ng_2^{2+}. (a) Analysis of electronic states along the dissociation coordinate in Ar_2^{2+} as calculated at the MRCI(10,11)/def2QZVPPD level. Solid and dashed lines refer to singlet and triplet states, respectively. (b)–(d) Dissociation curves in Ar_2^{2+}, Kr_2^{2+}, and Xe_2^{2+} as calculated at the MRCI/def2QZVPPD level with (10,9) and (10,11) active spaces. Red arrows indicate the equilibrium bond length in Ng_2^{+}. See the ESI,† for numerical values (Table S6, ESI†) and benchmarking calculations on Xe_2^{2+} (Fig. S2, ESI†).

over a small barrier of about 0.1 eV and 0.3 eV for Kr_3^{2+} and Xe_3^{2+}, respectively (Table 1). However, the precise value of the barrier is affected considerably by parametrization of the MRCI method; from our benchmarks we suggest an error of the barrier energy of around 0.1 eV for Xe_3^{2+} arising from the active space size (see Fig. S3, ESI†). All MRCI calculations consistently predict a metastable bound structure for Kr_3^{2+} and Xe_3^{2+}.

4 Discussion

Isotopologues of dicationic dimers and trimers of Kr and Xe whose mass/charge ratio is half integer have been identified in high-resolution mass spectra. Their appearance implies that they have survived intact from the time of ion extraction until the reflectron in the TOF-MS, which measures about 200–300 μs.

For Ar, Kr, and Xe, the calculated internuclear separation R_{TS} in the transition state of Ng_2^{2+} ($^1\Sigma_g^+$) exceeds the separation in the minimum of the ground state of Ng_2^{+} ($^2\Sigma_u^+$), see Table 1 and Fig. 3. Hence, a vertical transition from Ng_2^{+} ($^2\Sigma_u^+$) into Ng_2^{2+} ($^1\Sigma_g^+$) will likely end up to the left of the transition state in the PEC, resulting in a vibrationally excited quasi-bound dication. We do not know what the lifetime of these species with respect to tunneling would be in vacuum, but their interaction with the HND offers a pathway for vibrational relaxation and stabilization. While HNDs often fail to suppress ionization-induced fragmentation,[45–47] there are notable exceptions.[48,49] An ion formed on an attractive part of the PEC has more time for vibrational relaxation than one that is formed on a purely repulsive part.

Our mass spectra of Kr and Xe-doped HNDs reveal the presence of dicationic trimers which have so far not been observed for any noble gas. There are several factors that favor their formation from the monocations as opposed to from the neutral. First, the dications are linear symmetric molecules like their singly charged counterparts.[50] Second, the bond length in the dication is not much shorter than in monocation (2.91 Å *versus* 3.25 Å for Xe); again, when Ng_3^{+} is ionized to form Ng_3^{2+}, it would reach the part of the potential energy surface from which it can reach the metastable minimum (Fig. 4b and c). In contrast, the neutral trimer would have an equilateral geometry with a bond length of about 4.36 Å;[51] the Franck–Condon factor for a transition into the region of the metastable potential well of Ng_3^{2+} would be negligible.

We do not observe dicationic tetramers, nor slightly larger dications. An *ab initio* study of dicationic helium clusters has suggested quasistable He_n^{2+} up to n = 6, with a covalently bound trimer or tetramer core.[44] We succeeded to optimize a Xe_4^{2+} ion of a linear structure at the CCSD/def2TZVP level, with bond lengths of 3.11, 3.02, and 3.11 Å. The question is, though,

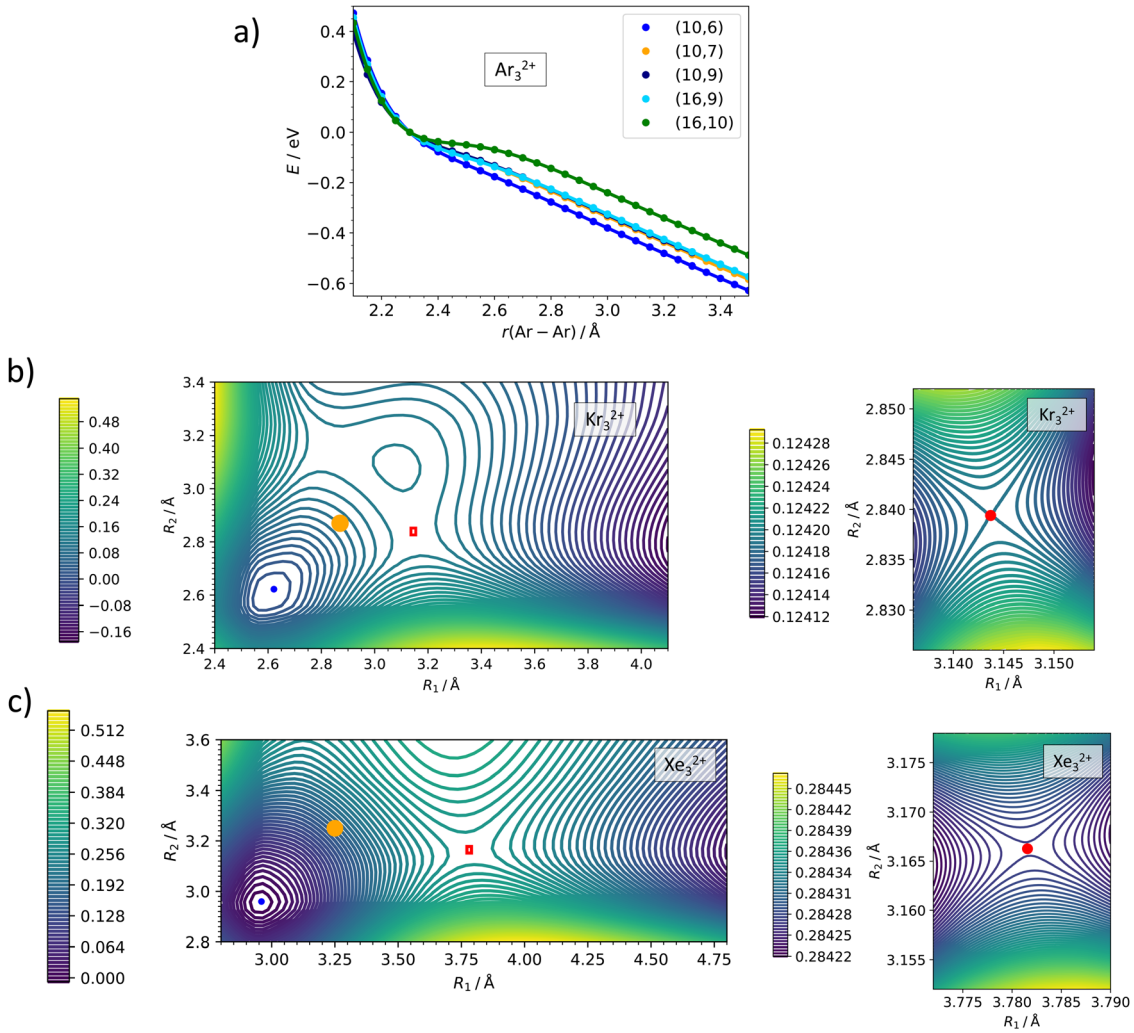

Fig. 4 Multi-reference calculations on Ng_3^{2+}. (a) Analysis of instability of Ar_3^{2+} as calculated at the MRCI/def2QZVPPD level with various active spaces. (b) and (c) Two-dimensional contour plots for dissociation of Kr_3^{2+} and Xe_3^{2+} as calculated at the MRCI(16,10)/def2QZVPPD level. Orange points show the optimal bond lengths in Ng_3^{+}, red rectangles show the region of the zoomed plot, red points the position of the transition state. See the ESI,† for benchmarking calculations on Xe_3^{2+} (Fig. S3, ESI†).

how fast charge transfer would lead to two separate charge centers within the complex, which would then quickly undergo fission into two singly charged clusters unless they contain dozens of atoms.[52,53] For Xe, for example, dicationic clusters containing at least 47 atoms have been observed upon electron ionization of neutral clusters.[54] With the current experimental approach we observe Xe_n^{2+} containing as few as 25 atoms if the HNDs are heavily doped, but no dications appear between n = 3 and 25. These findings will be reported in a future paper.

We have no direct information about the processes that occur in the doped HNDs when passing through the second ionizer or the collision cell where excess helium is being removed. We do not know for sure what the singly charged precursors of the observed dicationic dimers and trimers are. Ionization-induced fragmentation is a ubiquitous phenomenon in cluster science. It is conceivable that Ng atoms were lost upon formation of a long-lived dication Ng_n^{2+}, n = 2, 3.

Another issue is the mechanism by which dications are formed in the second ionization region. Broadly speaking, there are three pathways by which an incident electron may ionize a doped HND. First, the electron may directly ionize the dopant. Second, the incident electron may form He^+ which moves toward the dopant by resonant charge hopping and ionizes the dopant by charge transfer (or the charge may be trapped on He_2^+ which then migrates towards the dopant). Third, the incident electron may electronically excite the helium, and the dopant is ionized by an intracluster Penning mechanism.

The efficiency of process (1) is small compared to (2) and (3) unless the droplet is very small. Process (2) dominates if the dopant is heliophilic, but it can be excluded in the situation considered here because the charged dopant will repel He^+. Penning ionization (process 3) *via* formation of He* or He_2^* dominates if the dopant is heliophobic and resides on the surface.[35,37–39] In a multiply charged droplet, the dopant ions reside close to the surface because of Coulomb repulsion, but

they will be surrounded by one or a few solvation layers.[36] Hence, it is not clear if heliophobic He* or He_2^* will be able to Penning ionize the dopant ions. However, photoelectron experiments of HNDs doped with noble gas atoms (which are heliophilic) have shown that Penning ionization does occur in small HNDs if the incident radiation leads to excitation of the 1s2p or higher bands.[55–57] A better understanding of the ionization mechanism could be obtained if the ion yield were to be measured *versus* the energy of the incident electrons, but this kind of experiment would require higher ion yields than attainable right now.

Finally we discuss the non-observation of doubly charged argon complexes which may be due to technical reasons. First, extraction of ions that exit from the He collision cell is disfavored for light ions with m/z well below 100. Second, the isotope pattern of argon disfavors mass spectrometric detection of dications. The Ar isotopes and their abundances are ^{36}Ar (0.34%), ^{38}Ar (0.06%), ^{40}Ar (99.90%). Thus, neither Ar_2^{2+} nor Ar_3^{2+} have any isotopologues with a half-integer m/z value. In summary, the absence of doubly charged Ar dimers or trimers in the current work conveys no definitive information about their stability or lack thereof.

5 Conclusions

We report the observation of Kr_2^{2+}, Kr_3^{2+}, Xe_2^{2+}, and Xe_3^{2+} in helium nanodroplets *via* post-ionization of singly-charged ions. Computational investigations suggest that when Ng_2^+ or Ng_3^+ is ionized, one reaches the potential energy surface in the region where doubly-charged ions are metastable, and dissociation is prevented by a small Coulomb barrier. Notably, the Coulomb barrier in Kr_3^{2+} is predicted to be around 0.1 eV, the ions are thus very efficiently stabilized by helium evaporation. We observed neither Ar_2^{2+} nor Ar_3^{2+}, although our *ab initio* calculations predict Ar_2^{2+} to be metastable with a considerable Coulomb barrier of 0.4 eV, preventing dissociation into $Ar^+ + Ar^+$. Most importantly, we have shown that our method of sequential double ionization can successfully prepare metastable, multiply-charged ions that would be hard or even impossible to form in other experimental approaches.

Data availability

The data that support the findings of this study are available from the corresponding authors upon reasonable request.

Author contributions

Conceptualization, E. G. (E. Gruber) and P. S. (P. Scheier); formal analysis, I. S. (I. Stromberg), S. B. (S. Bergmeister), M. M. D. (M. Mahmoodi-Darian), and E. G.; funding acquisition, M. O. (M. Ončák) and P. S.; investigation, I. S., S. B., E. G., G. S. (G. Schöpfer) and M. O.; methodology, E. G., M. O. and P. S.; project administration, M. O. and P. S.; resources, M. O. and P. S.; software, G. S. and M. O.; supervision, E. G., P. S. and M. O.; visualization, I. S., E. G., M. O. and O. E.; writing—original draft, M. O. and O. E.; writing—review & editing, I. S., S. B., E. G., M. M. D., G. S., M. O., P. S. and O. E. All authors have read and agreed to the published version of the manuscript.

Conflicts of interest

We declare no conflict of interest.

Acknowledgements

This work was supported by the Austrian Science Fund, projects Nr. P35013, T1181 and W1259. I. S. acknowledges financial support from Erasmus+ to support a student exchange year in Innsbruck. G. S. acknowledges receipt of a DOC Fellowship of the Austrian Academy of Sciences at the Institute of Ion Physics and Applied Physics at the University of Innsbruck. The computational results presented have been achieved using the HPC Infrastructure LEO of the University of Innsbruck. This article is based upon work from the COST Actions CA21101 – Confined Molecular Systems: From a New Generation of Materials to the Stars (COSY), supported by COST (European Cooperation in Science and Technology).

References

1 L. Pauling, The Normal State of the Helium Molecule-Ions He^{2+} and He^{2++}, *J. Chem. Phys.*, 1933, **1**, 56–59.
2 M. Guilhaus, A. G. Brenton, J. H. Beynon, M. Rabrenovic and P. von Rague Schleyer, First observation of He_2^{2+}: charge stripping of He^{2+} using a double-focusing mass spectrometer, *J. Phys. B*, 1984, **17**, L605.
3 M. Guilhaus, A. G. Brenton, J. H. Beynon, M. Rabrenović and P. von Ragué Schleyer, He_2^{2+}, the experimental detection of a remarkable molecule, *J. Chem. Soc., Chem. Commun.*, 1985, 210–211.
4 A. Belkacem, E. P. Kanter, R. E. Mitchell, Z. Vager and B. J. Zabransky, Measurement of the ultrashort bond length in He^{2++}, *Phys. Rev. Lett.*, 1989, **63**, 2555–2558.
5 I. Ben-Itzhak, I. Gertner, D. Bortman and D. Zajfman, Formation of doubly charged molecular ion Ne_2^{2+} in sub-MeV stripping collision $Ne^{2+} + Ar \rightarrow Ne_2^{2+}$, *Phys. Rev. A: At., Mol., Opt. Phys.*, 1990, **41**, 6548–6551.
6 T. Tessner, W. Drachsel, J. Dirks and J. H. Block, Observation of doubly charged Ne_2 molecular ions by field desorption, *Int. J. Mass Spectrom. Ion Processes*, 1994, **134**, 161–168.
7 J. Ackermann and H. Hogreve, On the metastability of the $^1\Sigma_g^+$ ground state of He_2^{2+} and Ne_2^{2+}: a case study of binding metamorphosis, *J. Phys. B*, 1992, **25**, 4069.
8 J. Ackermann and H. Hogreve, Stability and spectral properties of the dication Ne_2^{2+}, *Phys. Chem. Chem. Phys.*, 2017, **19**, 32433–32442.

9 F. Fantuzzi, T. M. Cardozo and M. A. C. Nascimento, On the metastability of doubly charged homonuclear diatomics, *Phys. Chem. Chem. Phys.*, 2017, **19**, 19352–19359.
10 F. Grandinetti, Gas-Phase Ion Chemistry of the Noble Gases: Recent Advances and Future Perspectives, *Eur. J. Mass Spectrom.*, 2011, **17**, 423–463.
11 T. Jahnke, U. Hergenhahn, B. Winter, R. Dörner, U. Frühling, P. V. Demekhin, K. Gokhberg, L. S. Cederbaum, A. Ehresmann, A. Knie and A. Dreuw, Interatomic and Intermolecular Coulombic Decay, *Chem. Rev.*, 2020, **120**, 11295–11369.
12 N. Saito, Y. Morishita, I. H. Suzuki, S. D. Stoychev, A. I. Kuleff, L. S. Cederbaum, X.-J. Liu, H. Fukuzawa, G. Prümper and K. Ueda, Evidence of radiative charge transfer in argon dimers, *Chem. Phys. Lett.*, 2007, **441**, 16–19.
13 M. Lezius, S. Dobosz, D. Normand and M. Schmidt, Explosion Dynamics of Rare Gas Clusters in Strong Laser Fields, *Phys. Rev. Lett.*, 1998, **80**, 261–264.
14 B. Manschwetus, H. Rottke, G. Steinmeyer, L. Foucar, A. Czasch, H. Schmidt-Böcking and W. Sandner, Mechanisms underlying strong-field double ionization of argon dimers, *Phys. Rev. A: At., Mol., Opt. Phys.*, 2010, **82**, 13413.
15 J. Matsumoto, A. Leredde, X. Flechard, K. Hayakawa, H. Shiromaru, J. Rangama, C. L. Zhou, S. Guillous, D. Hennecart, T. Muranaka, A. Mery, B. Gervais and A. Cassimi, Asymmetry in Multiple-Electron Capture Revealed by Radiative Charge Transfer in Ar Dimers, *Phys. Rev. Lett.*, 2010, **105**, 263202.
16 Y. Morishita, X.-J. Liu, N. Saito, T. Lischke, M. Kato, G. Prümper, M. Oura, H. Yamaoka, Y. Tamenori, I. H. Suzuki and K. Ueda, Experimental Evidence of Interatomic Coulombic Decay from the Auger Final States in Argon Dimers, *Phys. Rev. Lett.*, 2006, **96**, 243402.
17 X. Ren, E. Jabbour Al Maalouf, A. Dorn and S. Denifl, Direct evidence of two interatomic relaxation mechanisms in argon dimers ionized by electron impact, *Nat. Commun.*, 2016, **7**, 11093.
18 E. Rühl, Core level excitation, ionization, relaxation, and fragmentation of free clusters, *Int. J. Mass Spectrom.*, 2003, **229**, 117–142.
19 J. Wu, A. Vredenborg, B. Ulrich, L. P. H. Schmidt, M. Meckel, S. Voss, H. Sann, H. Kim, T. Jahnke and R. Dörner, Multiple Recapture of Electrons in Multiple Ionization of the Argon Dimer by a Strong Laser Field, *Phys. Rev. Lett.*, 2011, **107**, 43003.
20 X. L. Zhu, S. Yan, W. T. Feng, X. Ma, X. Y. Chuai, D. L. Guo, Y. Gao, R. T. Zhang, P. Zhang, S. F. Zhang, D. M. Zhao, S. Xu, H. B. Wang, Z. K. Huang and D. B. Qian, Orientation effect in Ar dimer fragmentation by highly charged ion impact, *J. Phys. B*, 2018, **51**, 155204.
21 J. Ackermann and H. Hogreve, A CI study of quasi-bound Ar_2^{2+}, *Chem. Phys. Lett.*, 1993, **202**, 23–32.
22 C. Cachoncinlle, J. M. Pouvesle, G. Durand and F. Spiegelmann, Theoretical study of the electronic structure of Ar^{2++}, *J. Chem. Phys.*, 1992, **96**, 6085–6092.
23 P. Lablanquie, T. Aoto, Y. Hikosaka, Y. Morioka, F. Penent and K. Ito, Appearance of interatomic Coulombic decay in Ar, Kr, and Xe homonuclear dimers, *J. Chem. Phys.*, 2007, **127**, 154323.
24 M. Hoener, C. Bostedt, S. Schorb, H. Thomas, L. Foucar, O. Jagutzki, H. Schmidt-Böcking, R. Dörner and T. Möller, From fission to explosion: momentum-resolved survey over the Rayleigh instability barrier, *Phys. Rev. A: At., Mol., Opt. Phys.*, 2008, **78**, 21201.
25 D. Mathur and F. A. Rajgara, Communication: Ionization and Coulomb explosion of Xenon clusters by intense, few-cycle laser pulses, *J. Chem. Phys.*, 2010, **133**, 61101.
26 H. Murakami, H. Iwayama, K. Nagaya and M. Yao, Fragmentation channels of K-shell excited rare-gas clusters studied by multiple-ion coincidence momentum imaging, *J. Chem. Phys.*, 2008, **128**, 54303.
27 A. B. Treshchalov and A. A. Lissovski, Multi-band spectral structure and kinetics of the third continua in Ar, Kr and Xe gases excited by a pulsed discharge, *Eur. Phys. J. D*, 2012, **66**, 95.
28 S. Albertini, S. Bergmeister, F. Laimer, P. Martini, E. Gruber, F. Zappa, M. Ončák, P. Scheier and O. Echt, SF_6^+: Stabilizing Transient Ions in Helium Nanodroplets, *J. Phys. Chem. Lett.*, 2021, **12**, 4112–4117.
29 E. Gruber, S. Kollotzek, S. Bergmeister, F. Zappa, M. Ončák, P. Scheier and O. Echt, Phenanthrene: establishing lower and upper bounds to the binding energy of a very weakly bound anion, *Phys. Chem. Chem. Phys.*, 2022, **24**, 5138–5143.
30 S. Kollotzek, F. Izadi, M. Meyer, S. Bergmeister, F. Zappa, S. Denifl, O. Echt, P. Scheier and E. Gruber, Stabilization of phenanthrene anions in helium nanodroplets, *Phys. Chem. Chem. Phys.*, 2022, **24**, 11662–11667.
31 L. Ganner, S. Bergmeister, L. Lorenz, M. Ončák, P. Scheier and E. Gruber, Charging up the cold: formation of doubly- and triply-charged fullerene dimers in superfluid helium nanodroplets, *arXiv*, 2024, preprint, arXiv:2312.05151, DOI: **10.48550/arXiv.2312.05151**.
32 S. Bergmeister, L. Ganner, J. Locher, F. Zappa, P. Scheier and E. Gruber, Spectroscopy of helium-tagged molecular ions—Development of a novel experimental setup, *Rev. Sci. Instrum.*, 2023, **94**, 55105.
33 F. Laimer, L. Kranabetter, L. Tiefenthaler, S. Albertini, F. Zappa, A. M. Ellis, M. Gatchell and P. Scheier, Highly Charged Droplets of Superfluid Helium, *Phys. Rev. Lett.*, 2019, **123**, 165301.
34 D. Mateo and J. Eloranta, Solvation of Intrinsic Positive Charge in Superfluid Helium, *J. Phys. Chem. A*, 2014, **118**, 6407–6415.
35 A. Mauracher, O. Echt, A. M. Ellis, S. Yang, D. K. Bohme, J. Postler, A. Kaiser, S. Denifl and P. Scheier, Cold physics and chemistry: collisions, ionization and reactions inside helium nanodroplets close to zero K, *Phys. Rep.*, 2018, **751**, 1–90.
36 A. J. Feinberg, F. Laimer, R. M. P. Tanyag, B. Senfftleben, Y. Ovcharenko, S. Dold, M. Gatchell, S. M. O. O'Connell-Lopez, S. Erukala, C. A. Saladrigas, B. W. Toulson, A. Hoffmann, B. Kamerin, R. Boll, A. Fanis, P. de, Grychtol, T. Mazza, J. Montano, K. Setoodehnia, D. Lomidze,

R. Hartmann, P. Schmidt, A. Ulmer, A. Colombo, M. Meyer, T. Möller, D. Rupp, O. Gessner, P. Scheier and A. F. Vilesov, X-ray diffractive imaging of highly ionized helium nanodroplets, *Phys. Rev. Res.*, 2022, **4**, L022063.

37 M. P. Ziemkiewicz, D. M. Neumark and O. Gessner, Ultrafast electronic dynamics in helium nanodroplets, *Int. Rev. Phys. Chem.*, 2015, **34**, 239–267.

38 A. A. Scheidemann, V. V. Kresin and H. Hess, Capture of lithium by ^{4}He clusters: surface adsorption, Penning ionization, and formation of $HeLi^+$, *J. Chem. Phys.*, 1997, **107**, 2839–2844.

39 H. Schöbel, P. Bartl, C. Leidlmair, M. Daxner, S. Zöttl, S. Denifl, T. D. Märk, P. Scheier, D. Spångberg, A. Mauracher and D. K. Bohme, Sequential Penning Ionization: Harvesting Energy with Ions, *Phys. Rev. Lett.*, 2010, **105**, 243402.

40 M. J. Frisch, G. W. Trucks, H. B. Schlegel, G. E. Scuseria, M. A. Robb, J. R. Cheeseman, G. Scalmani, V. Barone, G. A. Petersson, H. Nakatsuji, X. Li, M. Caricato, A. V. Marenich, J. Bloino, B. G. Janesko, R. Gomperts, B. Mennucci, H. P. Hratchian, J. V. Ortiz, A. F. Izmaylov, J. L. Sonnenberg, D. Williams-Young, F. Ding, F. Lipparini, F. Egidi, J. Goings, B. Peng, A. Petrone, T. Henderson, D. Ranasinghe, V. G. Zakrzewski, J. Gao, N. Rega, G. Zheng, W. Liang, M. Hada, M. Ehara, K. Toyota, R. Fukuda, J. Hasegawa, M. Ishida, T. Nakajima, Y. Honda, O. Kitao, H. Nakai, T. Vreven, K. Throssell, J. A. Montgomery Jr., J. E. Peralta, F. Ogliaro, M. J. Bearpark, J. J. Heyd, E. N. Brothers, K. N. Kudin, V. N. Staroverov, T. A. Keith, R. Kobayashi, J. Normand, K. Raghavachari, A. P. Rendell, J. C. Burant, S. S. Iyengar, J. Tomasi, M. Cossi, J. M. Millam, M. Klene, C. Adamo, R. Cammi, J. W. Ochterski, R. L. Martin, K. Morokuma, O. Farkas, J. B. Foresman and D. J. Fox, *Gaussian 16 Rev. A.03*, Gaussian Inc., Wallingford, CT, 2016.

41 H.-J. Werner, P. J. Knowles, G. Knizia, F. R. Manby and M. Schütz, Molpro: a general-purpose quantum chemistry program package, *Wiley Interdiscip. Rev.: Comput. Mol. Sci.*, 2012, **2**, 242–253.

42 H.-J. Werner, P. J. Knowles, R. Lindh, F. R. Manby, M. Schütz, P. Celani, T. Korona, A. Mitrushenkov, G. Rauhut, T. B. Adler, R. D. Amos, A. Bernhardsson, A. Berning, D. L. Cooper, M. J. O. Deegan, A. J. Dobbyn, F. Eckert, E. Goll, C. Hampel, G. Hetzer, T. Hrenar, G. Knizia, C. Köppl, Y. Liu, A. W. Lloyd, R. A. Mata, A. J. May, S. J. McNicholas, W. Meyer, M. E. Mura, A. Nicklaß, P. Palmieri, K. Pflüger, R. Pitzer, M. Reiher, U. Schumann, H. Stoll, A. J. Stone, R. Tarroni, T. Thorsteinsson, M. Wang and A. Wolf, *MOLPRO, version 2012.1, a Package of Ab Initio Programs*, Stuttgart, 2012, see **https://www.molpro.net**.

43 A. J. Johnsen, A. B. Alekseyev, G. G. Balint-Kurti, M. Brouard, A. Brown, R. J. Buenker, E. K. Campbell and D. B. Kokh, A complete quantum mechanical study of chlorine photodissociation, *J. Chem. Phys.*, 2012, **136**, 164310.

44 H. Hogreve, On the resonance structure of the adiabatic hypersurfaces of small doubly charged helium clusters He_n^{++}, n = 3–6, *J. Chem. Phys.*, 1992, **96**, 3010–3021.

45 M. Mudrich and F. Stienkemeier, Photoionisaton of pure and doped helium nanodroplets, *Int. Rev. Phys. Chem.*, 2014, **33**, 301–339.

46 H. Schöbel, P. Bartl, C. Leidlmair, S. Denifl, O. Echt, T. D. Märk and P. Scheier, High-resolution mass spectrometric study of pure helium droplets, and droplets doped with krypton, *Eur. Phys. J. D*, 2011, **63**, 209–214.

47 S. Yang, S. M. Brereton, M. D. Wheeler and A. M. Ellis, Soft or hard ionization of molecules in helium nanodroplets? An electron impact investigation of alcohols and ethers, *Phys. Chem. Chem. Phys.*, 2005, **7**, 4082–4088.

48 A. M. Ellis and S. F. Yang, Role of Helium Droplets in Mass Spectra of Diatomics: Suppression of Dissociative Reactions, *Chin. J. Chem. Phys.*, 2015, **28**, 489–492.

49 Y. Ren and V. V. Kresin, Suppressing the fragmentation of fragile molecules in helium nanodroplets by coembedding with water: possible role of the electric dipole moment, *J. Chem. Phys.*, 2008, **128**, 74303.

50 M. Daskalopoulou, H.-U. Böhmer and S. D. Peyerimhoff, Multi-reference configuration interaction calculations on the systems Xe_2^+ and Xe_3^+, *Z. Phys. D: At., Mol. Clusters*, 1990, **15**, 161–169.

51 P. J. Linstrom and W. G. Mallard, The NIST Chemistry WebBook: A Chemical Data Resource on the Internet, *J. Chem. Eng. Data*, 2001, **46**, 1059–1063.

52 O. Echt, D. Kreisle, E. Recknagel, J. J. Saenz, R. Casero and J. M. Soler, Dissociation channels of multiply charged van der Waals clusters, *Phys. Rev. A: At., Mol., Opt. Phys.*, 1988, **38**, 3236–3248.

53 O. Echt, P. Scheier and T. D. Märk, Multiply charged clusters, *C. R. Phys.*, 2002, **3**, 353–364.

54 P. Scheier and T. D. Märk, Doubly charged argon clusters and their critical size, *J. Chem. Phys.*, 1987, **86**, 3056–3057.

55 C. C. Wang, O. Kornilov, O. Gessner, J. H. Kim, D. S. Peterka and D. M. Neumark, Photoelectron imaging of helium droplets doped with Xe and Kr atoms, *J. Phys. Chem. A*, 2008, **112**, 9356–9365.

56 D. Buchta, S. R. Krishnan, N. B. Brauer, M. Drabbels, P. O'Keeffe, M. Devetta, M. Di Fraia, C. Callegari, R. Richter, M. Coreno, K. C. Prince, F. Stienkemeier, R. Moshammer and M. Mudrich, Charge Transfer and Penning Ionization of Dopants in or on Helium Nanodroplets Exposed to EUV Radiation, *J. Phys. Chem. A*, 2013, **117**, 4394–4403.

57 L. B. Latief, M. Shcherbinin, S. R. Krishnan, R. Richter, T. Pfeifer and M. Mudrich, Direct inner-shell photoionization of Xe atoms embedded in helium nanodroplets, *J. Phys. B*, 2020, **53**, 204001.

